

**Cylinder–flat-surface contact mechanics during sliding**J. Wang *PGI-1, FZ Jülich, Germany, European Union  
and College of Science, Zhongyuan University of Technology, Zhengzhou 450007, China*A. Tiwari \* and B. N. J. Persson\* †*PGI-1, FZ Jülich, Germany, European Union*I. M. Sivebaek *PGI-1, FZ Jülich, Germany, European Union;  
Department of Mechanical Engineering, Technical University of Denmark, Kongens Lyngby 2800, Denmark, European Union;  
and Novo Nordisk Device R & D, DK-3400 Hillerød, Denmark, European Union*

(Received 28 June 2020; accepted 16 September 2020; published 14 October 2020)

Using molecular dynamics we study the dependency of the contact mechanics on the sliding speed when an elastic block (cylinder) with a  $\cos(q_0x)$  surface height profile is sliding in adhesive contact on a rigid flat substrate. The atoms on the block interact with the substrate atoms by Lennard-Jones potentials, and we consider both commensurate and (nearly) incommensurate contacts. For the incommensurate system the friction force fluctuates between positive and negative values, with an amplitude proportional to the sliding speed, but with the average close to zero. For the commensurate system the (time-averaged) friction force is much larger and nearly velocity independent. For both types of systems the width of the contact region is velocity independent even when, for the commensurate case, the frictional shear stress increases from zero (before sliding) to  $\approx 0.1$  MPa during sliding. This frictional shear stress, and the elastic modulus used, are typical for polydimethylsiloxane rubber sliding on a glass surface, and we conclude that the reduction in the contact area observed in some experiments when increasing the tangential force must be due to effects not included in our model study, such as viscoelasticity or elastic nonlinearity.

DOI: [10.1103/PhysRevE.102.043002](https://doi.org/10.1103/PhysRevE.102.043002)**I. INTRODUCTION**

The contact between a spherical (or cylindrical) body and a flat surface is perhaps the simplest possible contact mechanics problem, and is often used in model studies of adhesion and friction [1–4]. For stationary contact with  $F_x = 0$ , where  $F_x$  is the applied tangential force, the adhesive interaction is well described by the Johnson-Kendall-Roberts (JKR) theory [5,6] which has been tested in great detail. However, when the tangential force  $F_x$  is nonzero, the problem becomes much more complex and not fully understood [7–12].

Here, we consider the contact between an elastic block with a cylinder shape with the height profile  $z = h_0 \cos(q_0x)$ , and a rigid solid with a flat surface. We will refer to this system as curved flat. In Refs. [11,12] we studied the opposite situation of an elastic block with a flat surface in contact with a rigid solid with the height profile  $z = h_0 \cos(q_0x)$ . We will refer to this system as flat curved. When  $F_x = 0$ , the curved-flat and flat-curved systems are both described by the JKR theory. However, as will be shown here, during sliding the two systems exhibit very different properties.

**II. MODEL**

A curved elastic block can be obtained by “gluing” an elastic slab to a rigid upper surface profile. Here, we use a slab of thickness  $L_z \approx 86$  Å attached to a rigid surface with the height profile  $z = h_0 \cos(q_0x)$ , where  $h_0 = 100$  Å and  $q_0 = 2\pi/L_x$ . During sliding we move the upper rigid profile of the block in the  $x$  direction (see Fig. 1) with a constant speed  $v$  while the normal force squeezing the block against the substrate (see below) is constant.

We use periodic boundary conditions in the  $xy$  plane with  $L_x = 254$  Å and  $L_y = 14$  Å. The number of atoms in the  $x$  direction is  $N_x = 128$  for the block, and for the substrate we consider two cases where  $N_x = 128$  (commensurate interface) and  $N_x = 206$ . In the latter case the ratio between the lattice constant of the block and the substrate is  $a_b/a_s = 206/128 \approx 1.609$ , which is close to the golden mean  $(1 + \sqrt{5})/2 \approx 1.618$ , i.e., the interface is nearly incommensurate. A picture showing the atoms at the interface before contact is shown in Fig. 1.

The elastic block is treated using the smart-block description (with 13 layers with the same spacing as for the first layer plus four layers on top of it, where at every step we double the lattice spacing in the  $x$  and  $z$  directions) discussed in Ref. [11], where the bending and elongation spring

\*[www.MultiscaleConsulting.com](http://www.MultiscaleConsulting.com)†Corresponding author: [b.persson@fz-juelich.de](mailto:b.persson@fz-juelich.de)

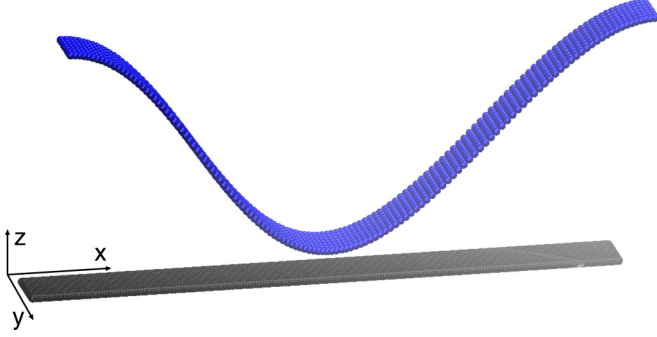


FIG. 1. Picture of the bottom layer of atoms on the block (blue) and the top layer of atoms on the substrate (black) before contact. We use periodic boundary conditions in the  $xy$  plane. The block is elastic and of thickness  $L_z \approx 86$  Å. The upper surface of the block is “glued” to a rigid surface with a cosine profile in the  $x$  direction.

constants are chosen to give the Young’s modulus and the Poisson ratio  $E = 10$  MPa and  $\nu = 0.5$ , respectively. The interaction potential between the block and wall atoms at the interface is of the Lennard-Jones (LJ) type,

$$V(r) = 4V_0 \left[ \left( \frac{r_0}{r} \right)^{12} - \left( \frac{r_0}{r} \right)^6 \right],$$

where  $V_0 = 0.04$  meV and  $r_0 = 3.28$  Å. With this interaction potential we calculate the (adiabatic) work of adhesion  $w \approx 0.0023$  J/m<sup>2</sup> for the commensurate interface, and  $w \approx 0.0027$  J/m<sup>2</sup> for the incommensurate interface. We note that in the present system, when the adhesion is removed ( $w \rightarrow 0$ ), the contact width decreases from 85.3 to 25.8 Å when the nominal pressure  $p = 0.1$  MPa, and from 101.1 to 61.5 Å when  $p = 1$  MPa. Thus, in spite of the small work of adhesion, the adhesion interaction is very important, which is due to the small size of the system [in the JKR theory the width of the contact region depends on the (dimensionless) parameter  $w/(pR)$ , where  $R$  is a length characterizing the size of the system;  $w/(pR)$  is of order unity in the present case].

Figure 2 shows for the incommensurate interface the system, in Fig. 2(a) before contact, and in Fig. 2(b) after squeezing the block against the substrate with the nominal contact pressure  $p = F_z/(L_x L_y) = 0.1$  MPa (blue), and  $p = 1$  MPa (red). We also show the contact for the flat-curved case studied in Refs. [11,12].

### III. NUMERICAL RESULTS

Figure 3 shows the friction coefficient  $\mu = F_x/F_z$  (green lines) and its (local) average (blue) as a function of the distance  $s = vt$  moved by the upper surface of the block for the (nearly) incommensurate [Fig. 3(a)] and the commensurate [Fig. 3(b)] system. The sliding speed  $v = 0.1$  m/s and the nominal contact pressure  $p = 0.1$  MPa. For the incommensurate system the average friction coefficient nearly vanishes ( $\mu < 10^{-4}$ ) while for the commensurate system it is of order unity ( $\mu \approx 0.9$ ). Note that there is nearly no drop in the friction force at the onset of sliding, i.e., the static and kinetic friction coefficients are nearly equal which we also observe for other sliding speeds.

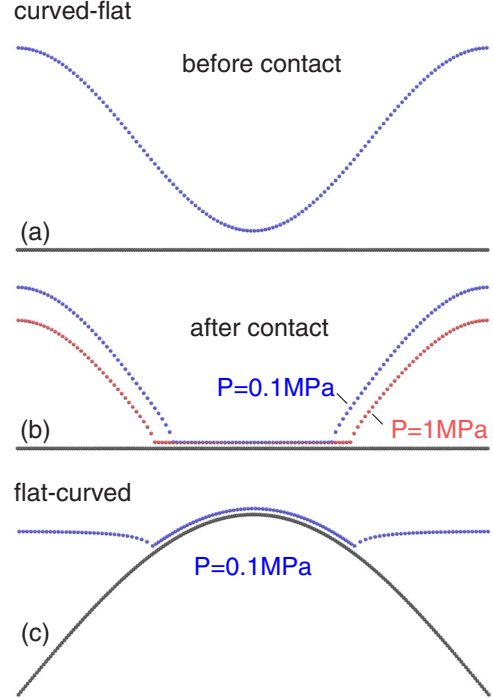


FIG. 2. Contact area between an elastic slab (block) and a rigid substrate at the temperature  $T = 0$  K. In (a) and (b) the block is corrugated with the height coordinate  $z = h_0 \cos(q_0 x)$  with  $q_0 = 2\pi/L_x$ . In (c) the substrate has the same corrugation amplitude but with a double wavelength (i.e.,  $q_0 = \pi/L_x$ ), while the block has a flat surface. We denote the two different systems as curved flat and flat curved. For the curved-flat system we show the contact (a) before and (b) after squeezing the block against the substrate with the nominal contact pressure  $p = 0.1$  MPa (blue), and  $p = 1$  MPa (red). For the flat-curved system we show the contact for the nominal contact pressure  $p = 0.1$  MPa. The Young’s modulus for the elastic block  $E = 10$  MPa, and the LJ block-substrate atom interaction parameters are given in the text.

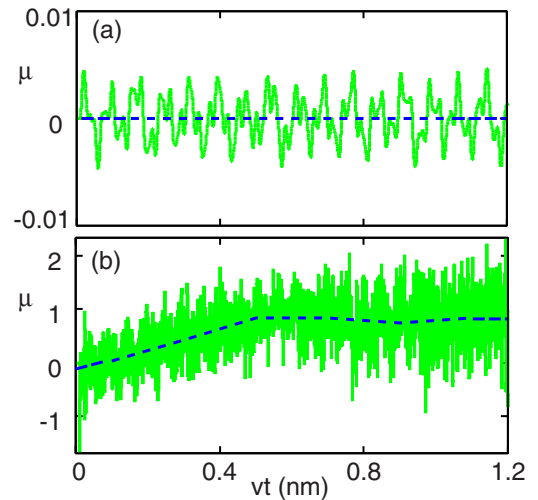


FIG. 3. The friction coefficient  $\mu = F_x/F_z$  as a function of the distance  $vt$  moved by the top of the elastic block (curved-flat system). For (a) the incommensurate and (b) the commensurate interface. The nominal contact pressure  $p = 0.1$  MPa and the speed  $v = 0.1$  m/s.

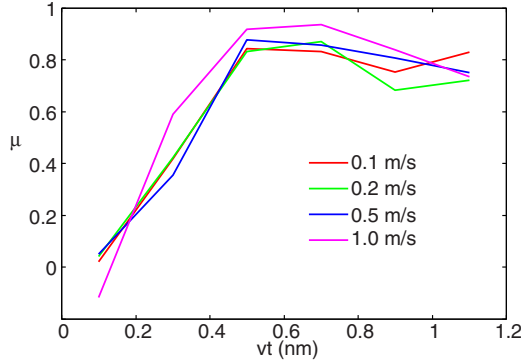


FIG. 4. The friction coefficient  $\mu = F_x/F_z$  as a function of the sliding distance for the commensurate system. The sliding speed  $v = 0.1, 0.2, 0.5,$  and  $1$  m/s, and the contact pressure  $p = 0.1$  MPa.

The oscillations in  $F_x/F_z$  for the incommensurate system are due to the abrupt start in sliding where the upper surface of the block abruptly starts to move with the speed  $v = 0.1$  m/s at time  $t = 0$  (see the movie [13]). This results in an elastic wave propagating [with the transverse sound velocity  $c_T = (G/\rho)^{1/2} \approx 56$  m/s] towards the interface so that only after the time  $t = d/c_T$  will the atoms at the interface start to move. The periodicity of the fluctuation in the tangential force  $F_x$  in Fig. 3(a) is given by the time it takes for an elastic wave to propagate back and forth between the two surfaces, i.e., the distance  $2d$  giving the time  $\Delta t = 2d/c_T$  or sliding distance  $\Delta s = v\Delta t = 2dv/c_T$ . Using  $v = 0.1$  m/s,  $c_T = 56$  m/s, and  $d = 8.6$  nm, this gives  $\Delta s = 0.031$  nm. The numerical calculations show that the period (in time) of the oscillations in  $F_x$  is independent of the sliding speed  $v$ , and the contact pressure  $p$ , while the amplitude of the oscillations is proportional to  $v$ .

For the commensurate interface the friction is much larger and nearly velocity independent (see Fig. 4). This is the expected result when at the sliding interface rapid slip events occur, involving velocities independent of the driving speed  $v$ . Observations of the movies (see Ref. [14]) show that the sliding motion involves domain-wall excitation (solitons), which propagate with high speed (of order of the Rayleigh sound velocity; see Fig. 5), unrelated to the sliding speed  $v$ , while energy is radiated into the block, giving rise to the observed high friction force.

For both the commensurate and the incommensurate systems the contact width does not change with sliding speed in the studied velocity range ( $v < 1$  m/s). For the incommensurate system this is expected because of the nearly vanishing (average) friction force, but for the commensurate system the friction is large but still the contact width is independent of the sliding speed. In particular, there is no change in the contact width between  $v = 0$  with  $F_x = 0$  and sliding at a finite velocity where the frictional shear stress is of order 0.1 MPa [as is typical for polydimethylsiloxane (PDMS) sliding on a glass surface [15]].

Earlier, we had studied sliding friction for the flat-curved situation where an elastic block with a smooth surface is sliding on a rigid surface with the height profile  $z = h_0 \cos(q_0x)$ . This case differs from the curved-flat configuration studied above since for the flat-curved system there is an impor-

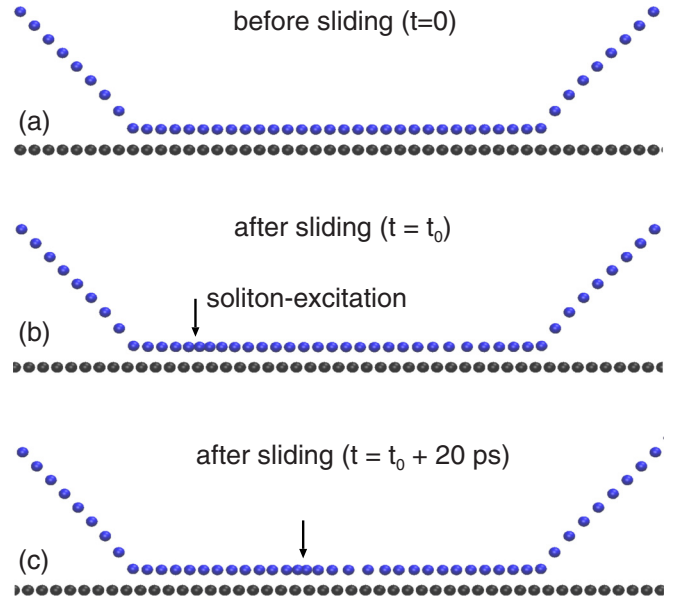


FIG. 5. For the curved-flat system with a commensurate interface the sliding motion consists of “long” time periods of no sliding followed by rapid slip events where the block moves forward by one substrate lattice spacing. The rapid motion consists of a compression domain wall (solitonlike excitation) which propagates with a velocity ( $\approx 43$  m/s) close to the Rayleigh sound velocity ( $\approx 0.95c_T \approx 53$  m/s). During this rapid motion, elastic waves (phonons) are radiated into the block which is the origin of the observed friction force.

tant contribution to the friction from phonon emission from the opening and closing crack tips. In fact, for the system sizes we have studied, for the flat-curved case, even for the commensurate interface the contact edge contribution to the friction is larger than the contribution from the internal region of the contact. This is illustrated in Fig. 6, which shows the nominal frictional shear stress  $F_x/(L_xL_y)$  as a function of the sliding distance for the flat-curved case with an incommensurate interface (red curve), and for the commensurate interface (blue curve). In the calculations we have assumed the nominal

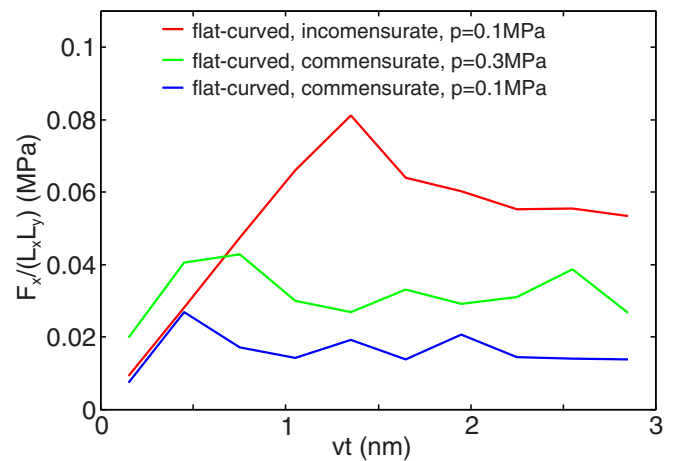


FIG. 6. The nominal shear stress as a function of the sliding distance for the flat-curved system with different communicabilities for the sliding speed  $v = 0.1$  m/s.

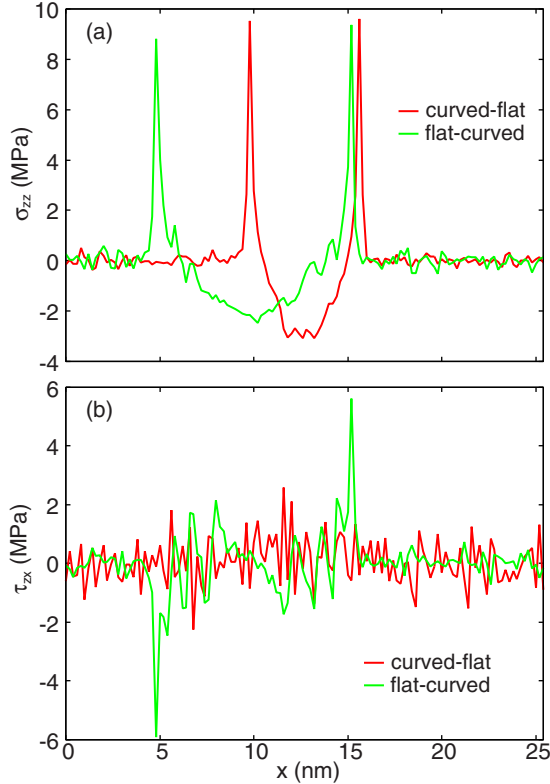


FIG. 7. (a) Normal stress  $\sigma_{zz}$  and (b) shear stress  $\tau_{xz}$  acting on the block as a function of the spatial coordinate  $x$ . For the curved-flat system (red curves), and for the flat-curved system (green curves), in both cases with a commensurate interface. The sliding speed  $v = 0.1$  m/s, and the nominal contact pressure  $p = 0.1$  MPa.

contact pressure  $p = 0.1$  MPa. The figure also shows the result for a higher contact pressure,  $p = 0.3$  MPa (green line). Note that the incommensurate interface gives the largest friction. For this system there is a negligible contribution to the friction from the internal region of the contact. That is, the friction is entirely due to the phonon emission associated with the rapid atomic snap-out and snap-in at the crack edges (see Refs. [11,12]). It is remarkable that the commensurate system gives lower friction than the incommensurate system, in spite of the fact that for this system there is both a contribution from the internal region of the contact and from the crack edges. However, the contribution from the crack edges is smaller than for the incommensurate system due to the higher density of substrate atoms for the incommensurate system (the ratio is  $206/128 \approx 1.61$ ).

Figure 7 shows the normal stress  $\sigma_{zz}$  [Fig. 7(a)] and the shear stress  $\tau_{xz}$  [Fig. 7(b)] acting on the block as a function of the spatial coordinate  $x$ . The red lines are for the curved-flat system, and the green lines for the flat-curved system, in both cases with a commensurate interface (with  $a_b/a_s = 128/128 = 1$ ). The sliding speed  $v = 0.1$  m/s, and the nominal contact pressure  $p = 0.1$  MPa. Note that in both cases at the edge of the contact region the normal stress  $\sigma_{zz}$  is tensile and maximal, as expected from the JKR theory, and from the theory of cracks, which predicts that the stress has an  $r^{-1/2}$  singularity at  $r = 0$  (where  $r$  is the distance from the crack tip). Because of the curved contact region in the

flat-curved system, at the edge of the contact region the stress  $\tau_{xz}$  will exhibit a similar singular form as the normal stress. However, for the curved-flat system the contact region is flat and only the  $\sigma_{zz}$  stress exhibits the singular form.

#### IV. DISCUSSION

We have shown above that within linear elasticity theory the contact area between an elastic cylinder and a rigid flat countersurface does not depend on the applied tangential force, at least not for the systems studied above. This is in contrast to some experimental results for PDMS spheres sliding on smooth glass surfaces. This indicates that the origin of the area reduction in the size of the contact area in Refs. [16–19] may be due to some effect not being taken into account in the model study, such as material viscoelasticity, elastic nonlinearity, or contact time-dependent work of adhesion.

In an interesting study Lengiewicz *et al.* [20] have found that the observed contact area reduction for a PDMS rubber sphere in contact with a glass surface can be explained by a theory based on nonlinear elasticity without invoking adhesion. They found quantitative agreement with the recent experimental results of Sahli *et al.* [17,18,20] on sphere-plane elastomer contacts, without adjustable parameters, using the neo-Hookean hyperelastic model. The importance of elastic nonlinearity for the explanation of the contact area reduction have been suggested by us in some earlier papers, in particular, in Ref. [21]. In another paper [11] we observed that for a dry, clean human finger there is no macroscopic adhesion to a flat glass plate (due to the large surface roughness of the skin), so the fact that for this case too the contact area is reduced upon application of a tangential force must clearly be a nonlinear elastic effect. That adhesion itself may not result in a reduction in the contact area upon application of a tangential force was also shown theoretically to be the case in the paper by Menga, Carbone, and Dini [9]. Finally, we note that in at least one study the rubber-glass contact area was found to increase upon sliding, indicating that other mechanisms may contribute to the dependency of the contact area on the tangential force [22].

If the reduction in the contact area upon application of a tangential force can be interpreted as an effective stiffening of the rubber elastic properties by the tangential deformations, then we expect also that the penetration is decreasing by increasing tangential force. This could explain the experimental observation in Ref. [21] that a sharp tip indented in a rubber surface with a given normal force moves upwards when a parallel force is applied in addition to the normal force. Within (small deformation) linear elasticity theory this result is unexpected as there is no coupling between the parallel and the perpendicular deformations when the Poisson ratio is equal to 0.5 (incompressible solid), as is the case in the rubbery region for rubberlike materials.

In this paper, and in Refs. [11,12], we have assumed simple crystalline solids. Rubberlike materials are more complex materials with cross-linked long-chain molecules, and may have nanometer-thick surface layers with liquidlike mobility of the polymer segments, which can rearrange in the substrate surface potential and form small regions which are pinned by the substrate. In this case, during lateral motion of the rubber

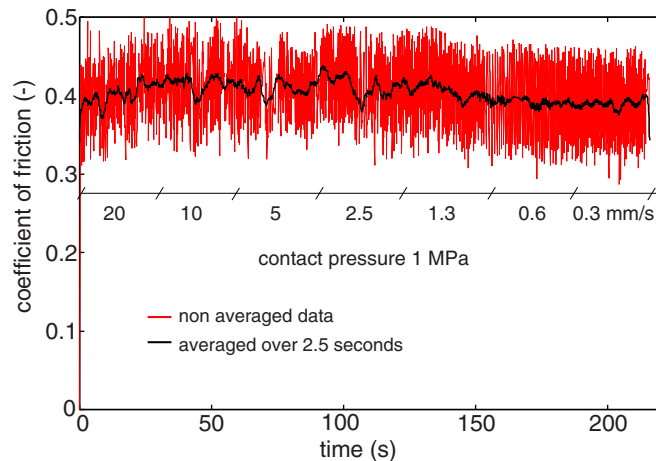


FIG. 8. The sliding friction for a polyoxymethylene (POM) polymer block sliding in a POM substrate. For a nominal flat interface with a nominal contact pressure 1 MPa and temperature  $T = 20^\circ\text{C}$ . See Ref. [28] for experimental details.

block, the chain stretches, detaches, relaxes, and reattaches to the surface to repeat the cycle. Here, “detaches” stands for the rearrangement of molecule segments (in small domains) parallel to the surface from pinned (commensurate-like) to depinned (incommensurate-like) domains. This results in an “area-dominated friction” where the shear stress is uniform within the contact area as observed experimentally [15]. In this case the friction force arises from a stick-slip type of motion of nanometer-sized regions everywhere within the contact region. Theoretical model studies of this process were presented in Refs. [23,24].

That systems with a (nearly) incommensurate interface exhibit smaller friction than systems with a commensurate interface, as found above, is well known, but in practice there are several “complications.” Thus, even if the interface is incommensurate, mobile adsorbed contamination molecules will always exist in the normal atmosphere, which will adjust their positions and pin the surfaces together, which may result in a large and nearly velocity-independent friction force [25,26]. Nevertheless, even if there are no strictly incommensurate systems, one expects a smaller friction force the closer an interface becomes to a perfect incommensurate system. As an example, if two polymers, say, A and B, with very different

natures of the bed units, slide on top of each other, a relatively small friction coefficient may prevail, while for A sliding on A, or B on B, the friction may be much higher due to the more commensurate-like contact [27,28]. In the latter cases the friction coefficient is also expected to be nearly velocity independent, assuming the sliding speed is not so high that frictional heating becomes important, or so low that thermal activation becomes important. As an example illustrating this, in Fig. 8 we show experimental results for the velocity dependency for a polyoxymethylene (POM) polymer block sliding on a POM substrate. Note that the friction coefficient is large ( $\mu \approx 0.4$ ) and nearly velocity independent.

## V. SUMMARY AND CONCLUSIONS

We have presented molecular dynamics simulations for an elastic cylinder sliding on a rigid flat countersurface (curved flat). For this system, within linear elasticity theory, the contact area does not depend on the applied tangential force.

The sliding friction of commensurate and incommensurate interface contacts was investigated. For the commensurate interface the friction is large and nearly velocity independent due to rapid slip events involving domain-wall excitation (solitons), which propagate at the interface with a speed of order of the sound velocity, radiating energy to the block, giving rise to the observed high friction force.

The geometry of contact, whether a curved-(rigid)flat contact or flat-(rigid)curved contact, decides the energy dissipation mechanism during sliding, resulting in the observed difference in frictional force. For the curved-flat case the friction force is mainly due to processes occurring inside the contact area, while for the flat-curved case, for the system we studied, the friction force is mainly due to phonon emissions at the crack edges associated with the rapid atom snap-out (at the opening crack) and snap-in (at the closing crack) events.

## ACKNOWLEDGMENT

J.W. is thankful for support via a scholarship from the China Scholarship Council (CSC) and funding by the National Natural Science Foundation of China (NSFC) Grant No. U1604131 and the training plan for young teachers in colleges and universities of Henan province, Grant No. 2017GGJS121.

- 
- [1] A. Tiwari, L. Dorogin, A. I. Bennett, K. D. Schulze, W. G. Sawyer, M. Tahir, and B. N. J. Persson, The effect of surface roughness and viscoelasticity on rubber adhesion, *Soft Matter* **13**, 3602 (2017).
  - [2] L. Dorogin, A. Tiwari, C. Rotella, P. Mangiagalli, and B. N. J. Persson, Role of Preload in Adhesion of Rough Surfaces, *Phys. Rev. Lett.* **118**, 238001 (2017).
  - [3] L. Dorogin, A. Tiwari, C. Rotella, P. Mangiagalli, and B. N. J. Persson, Adhesion between rubber and glass in dry and lubricated condition, *J. Chem. Phys.* **148**, 234702 (2018).
  - [4] H. Weiss, H.-W. Cheng, J. Mars, H. Li, C. Merola, F. U. Renner, V. Honkimäki, M. Valtiner, and M. Mezger, Structure and dynamics of confined liquids: Challenges and perspectives for the X-ray surface forces apparatus, *Langmuir* **35**, 16679 (2019).
  - [5] K. L. Johnson, K. Kendall, and A. D. Roberts, Surface energy and the contact of elastic solids, *Proc. R. Soc. London, Ser. A* **324**, 301 (1971).
  - [6] K. L. Johnson, *Contact Mechanics* (Cambridge University Press, Cambridge, UK, 1985).

- [7] A. R. Savkoor and G. A. D. Briggs, The effect of tangential force on the contact of elastic solids in adhesion, *Proc. R. Soc. London, Ser. A* **356**, 103 (1977).
- [8] K. L. Johnson, Adhesion and friction between a smooth elastic spherical asperity and a plane surface, *Proc. R. Soc. London, Ser. A* **453**, 163 (1997).
- [9] N. Menga, G. Carbone, and D. Dini, Do uniform tangential interfacial stresses enhance adhesion?, *J. Mech. Phys. Solids* **112**, 145 (2018); Corrigendum to “Do uniform tangential interfacial stresses enhance adhesion?” [Journal of the Mechanics and Physics of Solids **112**, 145 (2018)], **133**, 103774 (2019).
- [10] R. M. McMeeking, M. Ciavarella, G. Cricri, and K. S. Kim, The interaction of frictional slip and adhesion for a stiff sphere on a compliant substrate, *J. Appl. Mech.* **87**, 031016 (2020).
- [11] J. Wang, A. Tiwari, I. Sivebaek, and B. N. J. Persson, Sphere and cylinder contact mechanics during slip, *J. Mech. Phys. Solids* **143**, 104094 (2020).
- [12] J. Wang, A. Tiwari, I. M. Sivebaek, and B. N. J. Persson, Role of lattice trapping for sliding friction, *EPL* **131**, 24006 (2020).
- [13] Movie A: <https://youtu.be/kHQENBsFhPI>.
- [14] Movie B: <https://youtu.be/bTCaptUVzSY>; movie C: [https://youtu.be/PWjm6Q\\_NY](https://youtu.be/PWjm6Q_NY).
- [15] A. Chateauminis and C. Fretigny, Local friction at a sliding interface between an elastomer and a rigid spherical probe, *Eur. Phys. J. E* **27**, 221 (2008).
- [16] K. Vorvolakos and M. K. Chaudhury, The effects of molecular weight and temperature on the kinetic friction of silicone rubbers, *Langmuir* **19**, 6778 (2003).
- [17] R. Sahli, G. Pallares, C. Ducottet, I. E. Ben Ali, S. A. Akhrass, M. Guibert, and J. Scheibert, Evolution of real contact area under shear and the value of static friction of soft materials, *Proc. Natl. Acad. Sci. USA* **115**, 471 (2018).
- [18] R. Sahli, G. Pallares, A. Papangelo, M. Ciavarella, C. Ducottet, N. Ponthus, and J. Scheibert, Shear-Induced Anisotropy in Rough Elastomer Contact, *Phys. Rev. Lett.* **122**, 214301 (2019).
- [19] A. Papangelo, J. Scheibert, R. Sahli, G. Pallares, and M. Ciavarella, Shear-induced contact area anisotropy explained by a fracture mechanics model, *Phys. Rev. E* **99**, 053005 (2019).
- [20] J. Lengiewicz, M. de Souza, M. A. Lahmar, C. Courbon, D. Dalmas, S. Stupkiewicz, and J. Scheibert, Finite deformations govern the anisotropic shear-induced area reduction of soft elastic contacts, *J. Mech. Phys. Solids* **143**, 104056 (2020).
- [21] J. S. Persson, A. Tiwari, E. Valbabs, T. V. Tolpekina, and B. N. J. Persson, On the use of silicon rubber replica for surface topography studies, *Tribol. Lett.* **66**, 140 (2018).
- [22] B. A. Krick, J. R. Vail, B. N. J. Persson, and W. G. Sawyer, Optical in situ micro tribometer for analysis of real contact area for contact mechanics, adhesion, and sliding experiments, *Tribol. Lett.* **45**, 185 (2012).
- [23] A. Schallamach, A theory of dynamic rubber friction, *Wear* **6**, 375 (1963).
- [24] B. N. J. Persson and A. I. Volokitin, Rubber friction on smooth surfaces, *Eur. Phys. J. E* **21**, 69 (2006).
- [25] G. He and M. O. Robbins, Simulations of the kinetic friction due to adsorbed surface layers, *Tribol. Lett.* **10**, 7 (2001).
- [26] M. H. Müser, Nature of Mechanical Instabilities and their Effect on Kinetic Friction, *Phys. Rev. Lett.* **89**, 224301 (2002).
- [27] I. M. Sivebaek, V. N. Samoilov, and B. N. J. Persson, Frictional properties of confined polymers, *Eur. Phys. J. E* **27**, 37 (2008).
- [28] T. Ruby, T. J. Herslund, and I. M. Sivebaek, New tribotester for polymeric materials, in *Proceedings of the 12th Nordic Symposium on Tribology: NT2006-13-52, Helsingør, Denmark, June 7–9, 2006*, edited by P. Klit, S. Eskildsen, J. Jakobsen, and I. M. Sivebaek (Technical University of Denmark, Kongens Lyngby, 2006).